



Evaluation of the effectiveness of analytical models for cutting temperature in machining medium carbon steels under various cutting parameter combinations

F. Ramírez-Paredes* • V. Montenegro Simancas • F. Tapia Gudiño

Universidad Técnica del Norte, Facultad de Ingeniería en Ciencias Aplicadas, Ibarra, Ecuador

Received 12 08 2023; accepted 10 14 2024
Available 04 30 2025

Abstract: During the machining process, the temperature of the workpiece material has a direct effect on both the final product quality and the cutting tool life. The temperature increase can negatively affect the surface finish of the workpiece and safety risks during operation. On the other hand, excessively low temperatures can lead to higher cutting force and heightened friction between the tool and the workpiece. Then, accurate cutting temperature prediction has great importance in the production planning of machined parts. The temperature increase in the machined material is mainly due to the strain rate and the amount of deformed material. Cutting parameters that are directly associated with these factors include cutting speed, depth, feed rate, and tool geometry. In this study, they have proposed five models that consider different combinations of these machining parameters in a selective manner. The modeling process was carried out using a multivariate linear regression technique. These models are straightforward to implement and are applicable to various ranges of machining for medium-carbon steel. The results obtained from this study are satisfactory and align well with the reference experimental observations, demonstrating approximations in the range of 83-91%.

Keywords: Cutting temperatures, steel machining, carbon steel, orthogonal cutting, temperature modeling.

*Corresponding author.

E-mail address: frramirez@utn.edu.ec (F. Ramírez-Paredes).

Peer Review under the responsibility of Universidad Nacional Autónoma de México.

1. Introduction

Machining process study allows a better understanding of cutting mechanics. Considering the complexity of the cutting system, the most common methodologies are numerical methods and analytical cutting models. Variables like tool-chip contact temperature and residual stresses are difficult to measure directly, making estimation a more practical approach. This method enables the identification of the most significant factors in predicting these variables. (Ducobu et al., 2013)

In the machining process, macro variables such as cutting forces and material temperatures can be observed experimentally. These variables are closely related to the conversion of mechanical energy into heat. Their analysis is also performed through analytical models and numerical simulations. The key parameters in this process include cutting speed, feed rate, and cutting geometry (Yousefi & Zohoor, 2019).

Predicting cutting temperature has been a primary focus in metal cutting science due to its significant influence on tool wear and the quality of the machined surface (Ramírez et al., 2017). In situ measurement methods during machining are crucial for observing the temperature differences between the tool and the workpiece. This temperature gradient leads to a critical variation in heat flow during the machining process (Ghafari-zadeh et al., 2016).

Experimental analysis of cutting temperature has been principally focused on the use of thermocouples (CT) and infrared imaging (IR) (Battaglia et al., 2001). Currently, the finite element method (FEM) is the most widely used technique for simulating machining processes, accounting for the material's temperature-dependent behavior. This method enables the estimation of deformations, strain rates, stresses, and temperatures (Lei et al., 1999). The numerical results have been compared with analytical models and experimental data, particularly at the contact interfaces and in the temperature distribution within the cutting tool, showing consistent trends (Barzegar & Ozlu, 2021; Uçak et al., 2020).

Various numerical methods, such as the finite difference method, have shown that cutting parameters significantly influence the temperature of both the cutting tool and the workpiece. Cutting speed plays a critical role due to its impact on the strain rate and relative speed at contact interfaces, leading to greater heat generation in deformation zones (Barzegar & Ozlu, 2021). A threshold in the thermo-mechanical behavior of metals has been observed, where deformation energy decreases, making cutting speed the most sensitive parameter for controlling maximum and average temperatures, especially at low speeds (Pal & Dasmahapatra, 2022). High strain rates also contribute to increased temperatures due to the energy released during material

plastic deformation, which can cause mechanical instability (Lee & Yeh, 2008; Maranhão et al., 2013).

Feed rate and depth of cut (DOC) are key factors in predicting cutting temperatures, as both influence heat generation. Feed rate affects tool-chip contact length and the secondary shear zone, while DOC, being dominant in material removal rate (MRR), increases heat, especially when it becomes larger than the feed rate (Mutyalu et al., 2021; Verma & Srivastava, 2022). Additionally, the cutting tool rake angle significantly impacts temperature, with experimental data showing that positive rake angles increase cutting temperature due to greater tool-chip contact (Çakır et al., 2012; Pal & Dasmahapatra, 2022; Saglam et al., 2006).

All the aforementioned demonstrate that cutting temperatures are influenced by cutting speed, feed, rake angle and deep of cut (Liu et al., 2020). However, the effectiveness of different parameter combinations for estimating these cutting temperatures has not been evaluated within a single study. This study presents the development of five temperature models with different combinations of parameters and shows their prediction effectiveness. The modeling process was conducted using a multivariate regression technique with experimental data from specialized literature. The work material was medium carbon non-alloy steel, with plain uncoated carbide cutting tools and an orthogonal cutting configuration.

2. Materials and methods

This study presents the process of modeling the cutting temperature T_c based on combinations of machining parameters in medium carbon steel cutting. To achieve this, an analysis of experimentally observed temperature trends was conducted. All experimental data used were obtained under an orthogonal cutting configuration using plain uncoated carbide tools. Figure 1 illustrates the configuration used for the analysis and modeling, along with the relevant variables: cutting speed V_c [m/min], the feed rate t_1 [mm], the rake angle α [$^\circ$] and its modification $\alpha_m = \pi(90 - \alpha)/180$ in radians, and the depth of cut w in [mm].

This analysis has been carried out based on two considerations: the Boothroyd hypothesis about cutting temperatures as a function of Thermal number $R_T^{1/2}$ and the experimental observations from different studies about the influence of the deep of cut w and rake angle α over cutting temperatures. $R_T = V_c t_1 / \alpha_T$, where V_c is cutting velocity, t_1 is the feed rate and α_T is the workpiece material thermal diffusivity (Al Huda et al., 2002; Boothroyd, 1963; Chu & Wallbank, 1998; Fazil et al., 2014; Rodríguez et al., 2011; Saglam et al., 2006).

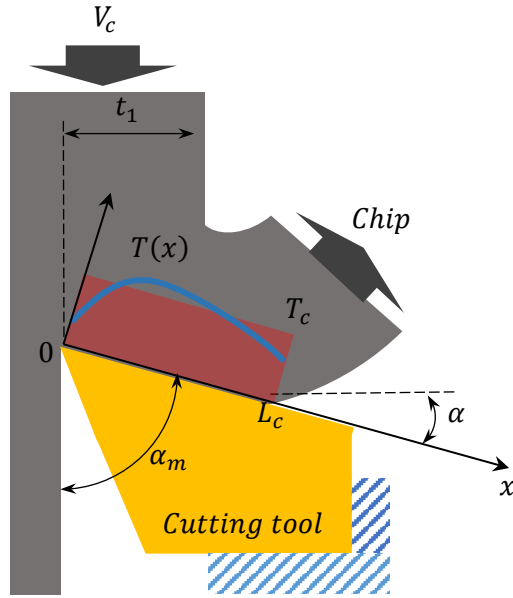
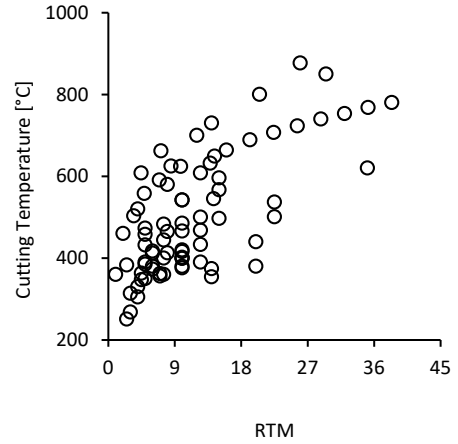


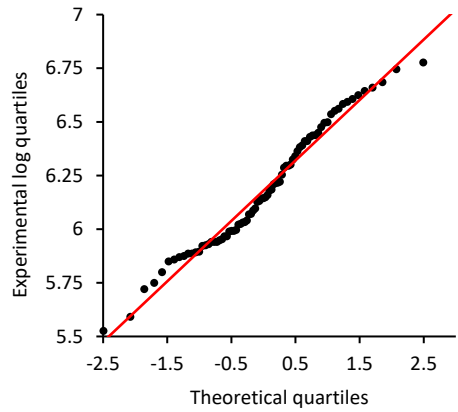
Figure 1. Orthogonal cutting configuration used in temperature modeling.

The experimental data used for the modeling and validation processes were obtained from high-impact specialized literature, under an orthogonal cutting configuration and consistent machining conditions. This ensures that the cutting temperature values obtained are comparable. All tests were conducted without cooling or lubrication, using flat uncoated carbide tools. The effect of the cutting-edge radius (CER) on cutting temperature decreases as the feed rate decreases. However, its influence on average cutting temperature is negligible for CER values below 40 [μm] (Emamian, 2018; Mane et al., 2019).

The temperature dataset used in the model development is shown in Figure 2(a), and its normality is presented in Figure 2(b). In the analysis of cutting temperature trends, the variable $R_{TM} = R_T \alpha_T \alpha_m$ was used, where R_T is the thermal number explained earlier, α_T represents the thermal conductivity of medium carbon steel, and α_m is the modified rake angle (Figure 1). The modeling ranges are as follows: cutting speed $V_c = 30 - 300 [m/min]$, feed rate $t_1 = 0.01 - 0.26 [mm]$, rake angle $\alpha = -10^\circ - +30^\circ$, and depth of cut $w = 0.1 - 3 [mm]$.



(a)



(b)

Figure 2. Temperature data used in modeling (Attanasio et al., 2008; Grzesik, 2006; Kitagawa et al., 1997; Norouzifard & Hamed, 2014; Tanaka et al., 2007; Ulutan et al., 2009; Umbrello et al., 2007).

2.1. Modeling process

In order to analyze the influence of different parameters on cutting temperature and identify the most efficient combinations for its estimation, it is necessary to develop a mathematical model that accounts for these potential combinations. Based on experimental observation (Figure 2) and information from the specialized literature, a potential mathematical model has been proposed, as shown in Eq. (1).

$$T_c = k \cdot \prod_{j=1}^n (x_j)^{z_j} \tag{1}$$

Where k, z_j are calibration constants, and x_j represents the j -th machining parameter used as a modeling variable. Equation (2) shows that the relative variation in cutting temperature depends on the model's calibration constants and the relative variation of the machining parameters considered in the model. Additionally, it has been observed that this variation is additive, meaning it allows for analyzing the influence of each parameter, individually or in combination, on the cutting temperature. The constants z_i are dimensionless.

$$\frac{dT_c}{T_c} = \sum_{j=1}^n z_j \frac{dx_j}{x_j} \tag{2}$$

Based on Equation (2), this work proposes analyzing the influence of four variables — V_c, t_1, α_m and w — on the cutting temperature modeling, independently. Therefore, five models with their own sets of regression coefficients are generated, and Equation (1) is rewritten to obtain Equation (3).

$$T_{c,i} = k_i \cdot V_c^{z_{i1}} t_1^{z_{i2}} \alpha_m^{z_{i3}} w^{z_{i4}} \tag{3}$$

Where $T_{c,i}$ is the value of T_c estimated with the i -th proposed model; k_i, z_{ij} are calibration constants with $i = 1, 2, \dots, 5; j = 1, 2, \dots, 4$. The modeling variables V_c, t_1, α_m and w are cutting speed, feed rate, modified rake angle and depth of cut, respectively. The angle α_m is measured from the machined surface to the tool's rake face (see Figure 1). Thus, there is an angular factor with positive values.

Table 1 shows the configuration of constants used in the modeling process. Model 1 considers the influence of all the cutting parameters explained above. Models 2, 3, 4 and 5 consider one of the cutting parameters as a constant in the modeling: V_c, t_1, α_m and w , respectively. The null value of the constant z_{ij} indicates which of the parameters V_c, t_1, α_m or w is constant in the proposed model: **Model "i"** with $i = 2 \dots 5$.

Table 1. List of constants of the different models proposed.

| Model i | k_i | V_c | t_1 | α_m | w |
|-----------|-------|----------|----------|------------|----------|
| Model 1 | k_1 | z_{11} | z_{12} | z_{13} | z_{14} |
| Model 2 | k_2 | 0 | z_{22} | z_{23} | z_{24} |
| Model 3 | k_3 | z_{31} | 0 | z_{33} | z_{34} |
| Model 4 | k_4 | z_{41} | z_{42} | 0 | z_{44} |
| Model 5 | k_5 | z_{51} | z_{52} | z_{53} | 0 |

The modeling was performed using the multivariate least squares method. For a linear fitting, Equation (3) was transformed into Equation (4).

$$T_{c,i}^* = k_i^* + z_{i1}V_c^* + z_{i2}t_1^* + z_{i3}\alpha_m^* + z_{i4}w^* \tag{4}$$

Where $y^* = \ln(y)$. The modeling results are presented in Table 2. Once the calibration constants are determined, the models represented by Equation (3) can estimate T_c under various combinations of the parameters x_i .

Model 1 was calibrated using all experimental reference data. Model 2 was calibrated with a subset of data obtained with constant cutting speed ($z_{21} = 0$). In this way, Model 2 estimates T_c , without considering the effect of the variation of V_c . Models 3-5 were calibrated with subsets of data from the original reference. Model 3 considers constant t_1 ($z_{32} = 0$), Model 4 considers constant α_m ($z_{43} = 0$), and Model 5 considers constant depth of cut ($z_{54} = 0$). In this way, five models have been generated to predict T_c using different combinations of cutting parameters.

All models demonstrate statistical significance ($F < F_{critical}$), and the regressions meet their objectives within the dataset used for model development. Based on these results, the developed models were applied, and the outcomes were compared with the complete set of experimental values. This comparison highlights the consistency of the proposed models with experimental trends. Figure 3 presents this comparison, showing the values predicted by the models. Calibration data are represented by triangles (▲).

Table 2. Modeling results.

| Model i | k_i | z_{i1} | z_{i2} | z_{i3} | z_{i4} | R | R^2 | R^2adj | F | $F_{critical}$ |
|-----------|---------|----------|----------|----------|----------|-------|-------|----------|---------|----------------|
| 1 | 181,704 | 0,169 | 0,241 | 1,885 | -0,059 | 0,839 | 0,705 | 0,689 | 44,135 | 6,85E-19 |
| 2 | 373,423 | 0 | 0,243 | 2,162 | -0,130 | 0,854 | 0,730 | 0,687 | 17,084 | 1,26E-05 |
| 3 | 86,593 | 0,207 | 0 | 1,881 | -0,082 | 0,858 | 0,736 | 0,690 | 15,821 | 3,60E-05 |
| 4 | 357,210 | 0,217 | -0,016 | 0 | -0,606 | 0,996 | 0,991 | 0,989 | 348,719 | 1,26E-09 |
| 5 | 242,572 | 0,159 | 0,240 | 1,034 | 0 | 0,770 | 0,592 | 0,553 | 15,020 | 3,24E-06 |

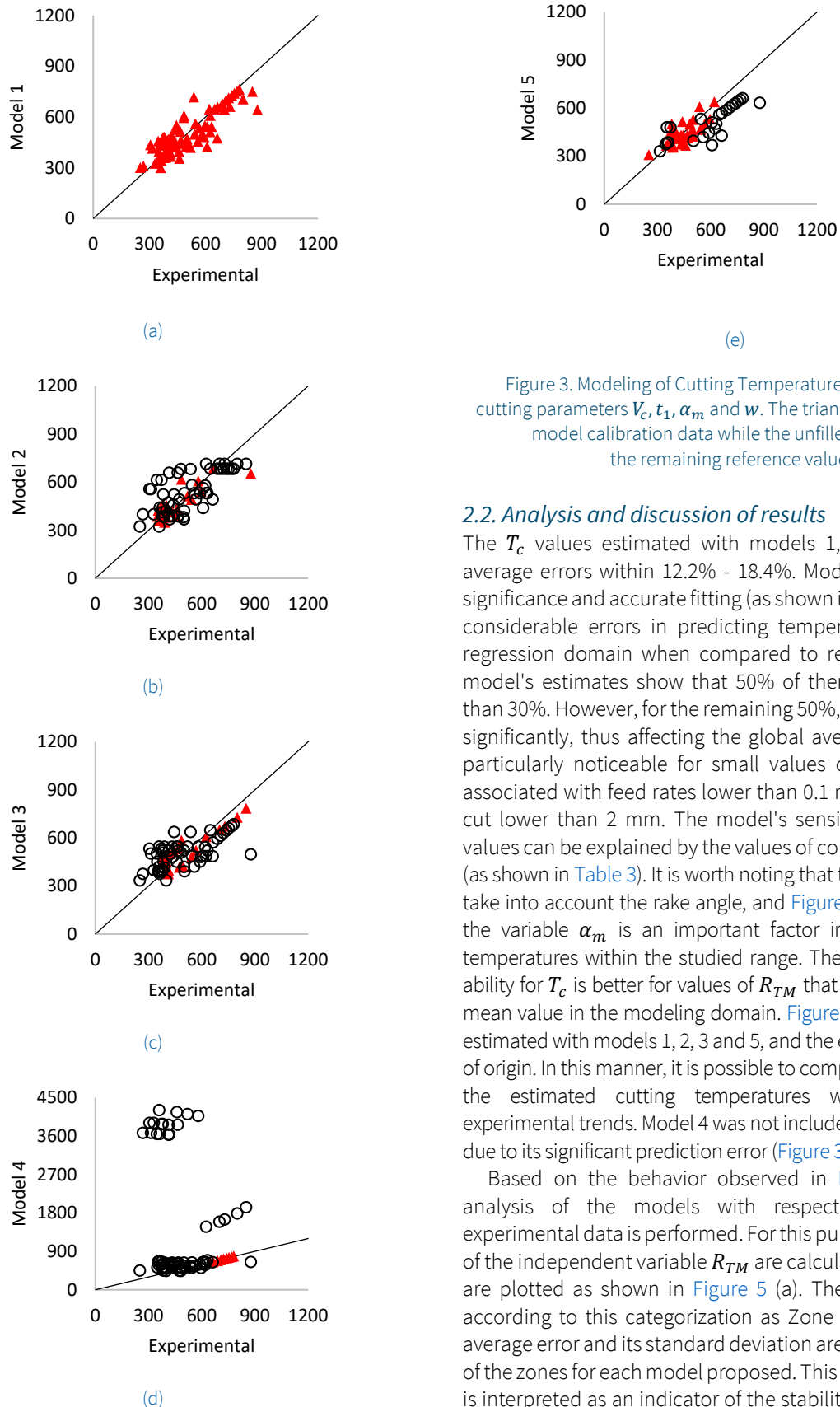


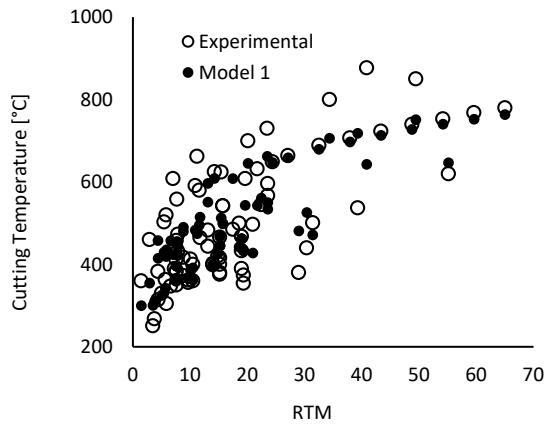
Figure 3. Modeling of Cutting Temperature T_c as a function of cutting parameters V_c , t_1 , α_m and w . The triangular points are the model calibration data while the unfilled points are the remaining reference values.

2.2. Analysis and discussion of results

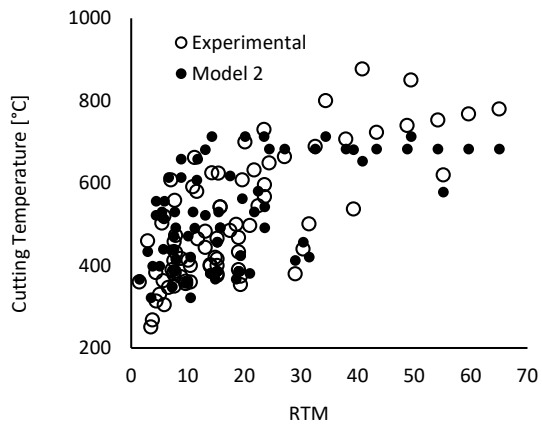
The T_c values estimated with models 1, 2, 3 and 5 show average errors within 12.2% - 18.4%. Model 4 has statistical significance and accurate fitting (as shown in Table 3), it shows considerable errors in predicting temperatures beyond its regression domain when compared to reference data. The model's estimates show that 50% of them have errors less than 30%. However, for the remaining 50%, the errors increase significantly, thus affecting the global average. This trend is particularly noticeable for small values of R_{TM} , which are associated with feed rates lower than 0.1 mm and a depth of cut lower than 2 mm. The model's sensitivity to these low values can be explained by the values of constants z_{42} and z_{44} (as shown in Table 3). It is worth noting that this model does not take into account the rake angle, and Figure 3 (d) suggests that the variable α_m is an important factor in modeling cutting temperatures within the studied range. The model's predictive ability for T_c is better for values of R_{TM} that are higher than the mean value in the modeling domain. Figure 4 shows the values estimated with models 1, 2, 3 and 5, and the experimental values of origin. In this manner, it is possible to compare the behavior of the estimated cutting temperatures with the reported experimental trends. Model 4 was not included in Figures 3 and 4 due to its significant prediction error (Figure 3 (d)).

Based on the behavior observed in Figure 4, an error analysis of the models with respect to the original experimental data is performed. For this purpose, the quartiles of the independent variable R_{TM} are calculated and the errors are plotted as shown in Figure 5 (a). The domain is zoned according to this categorization as Zone A, B, C, D and the average error and its standard deviation are calculated in each of the zones for each model proposed. This standard deviation is interpreted as an indicator of the stability of each model to predict T_c . The comparison of the average errors per model

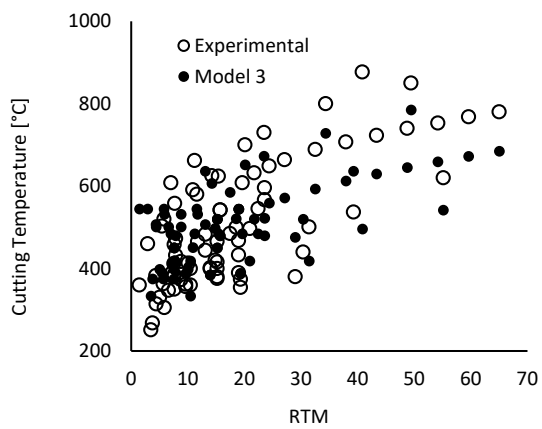
and per zone is shown in Figure 5 (b) and of the standard deviation in Figure 5 (c).



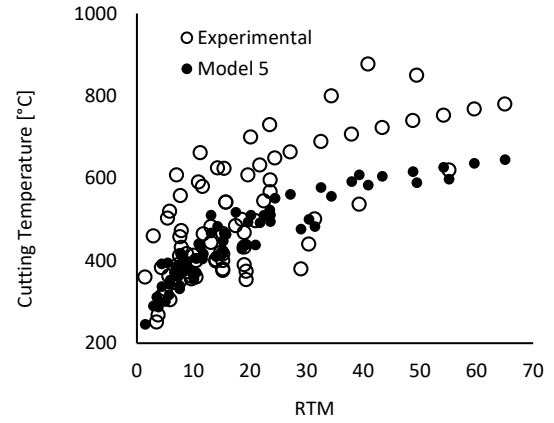
(a)



(b)

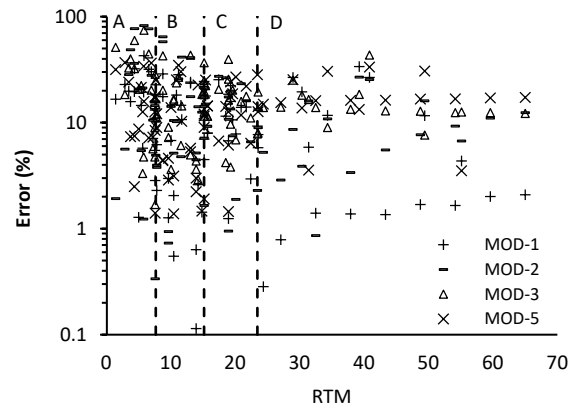


(c)

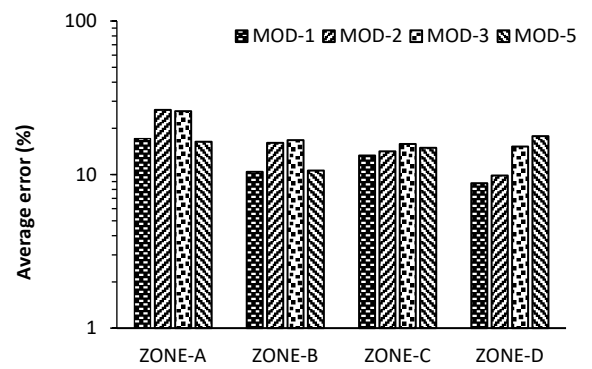


(d)

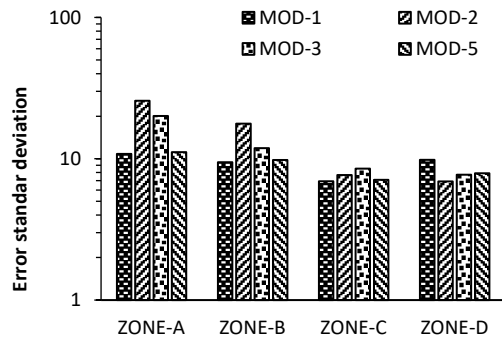
Figure 4. Cutting temperatures T_c obtained with the proposed models compared with the original modeling data.



(a)



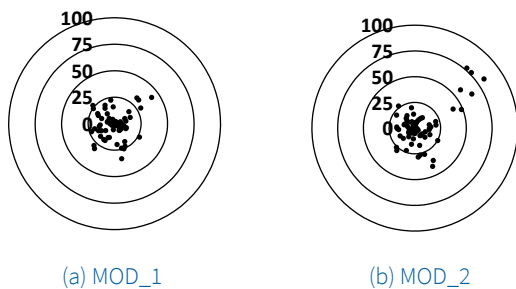
(b)



(c)

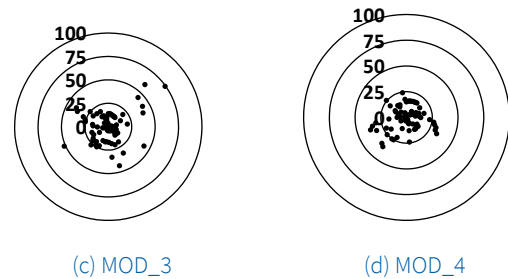
Figure 5. Error modeling analysis: (a) Error distribution of the models proposed. (b) Average error of approximation of each model in each analyzed area. (c) Standard deviation of error.

The error distribution presents values of 9 % to 26 % in all zones for models 1, 2, 3 and 5. Models 1 and 5 present the best prediction of T_c in the modeling domain (12% and 15%, respectively). A similar behavior is observed for the standard deviation in the four zones, with models 1 and 5 being the most stable with a dispersion of 9%. Figure 6 shows a comparison of the effectiveness of the models. If the density of points is focused on the center of Figures 6 (a)-(d), the model shows higher effectiveness in predicting T_c . This information is mostly qualitative. Figure 6 (e) instead shows the effectiveness of the five models in a quantitative way. To achieve this goal, three maximum error limits denoted by lines are used: 10%, 20%, and 30%. The vertical axis represents the percentage of measurements that comply with the maximum error percentage specified by each line. Specifically, for model 1, 95% of the predictions have an error rate lower than 30%, 81% of the predictions have an error rate lower than 20%, and 52% of the measurements have errors lower than 10% in comparison to the experimental values.



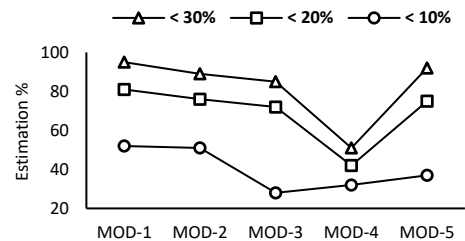
(a) MOD_1

(b) MOD_2



(c) MOD_3

(d) MOD_4



(e)

Figure 6. Effectiveness in the prediction of cutting temperatures.

It is observed that model 1 is more effective for $R_{TM} > 7.5$. Model 2 for $R_{TM} > 7$ or $t_1 < 0.1$. Model 3 improves its effectiveness for $R_{TM} > 10.5$. Model 5 improves its effectiveness with $R_{TM} > 5.5$. It is important to note that while the analyzed models conform to the domains outlined in R_{TM} , their effectiveness may be significantly reduced when operating at very low values of feed rate or depth of cut. Therefore, it is essential to consider this factor when the performance of these models is evaluated.

2.3. Validation of the models proposed

The T_c values estimated with models 1, 2, 3 and 5 show average errors within 12.2% - 18.4%.

After developing Models 1-5, they underwent a rigorous validation process. This involved comparing the temperature predictions with cutting temperatures derived from both validated theoretical models and experimental data, all under the same cutting conditions used for modeling. The goal of this validation was to ensure accuracy and reliability in predicting cutting temperatures. The validation was conducted in two phases: Phase A compared the developed models with established theoretical trends. While Phase B focused on comparing the models with experimental cutting temperature values obtained under conditions consistent with those used in the modeling process. This two-phase approach provided a thorough evaluation of the accuracy and effectiveness of the models in predicting cutting temperatures.

The theoretical reference trends for the validation of the proposed models (Phase A), correspond to the models shown in Table 3. These models have been validated in the specialized literature for medium carbon steel and ranges of $V_c = 50 - 300 [m/min]$, $t_1 = 0.05 - 0.45 [mm]$ and $w = 0.3 - 2.5 [mm]$. These models are functions of machining parameters and material characteristics (Fazil et al., 2014; Rodríguez et al., 2011).

The models used in this validation phase were proposed for oblique and orthogonal cutting. However, both models allow for the validation of the trends in the models proposed in this work, as it has been experimentally observed that the maximum and average temperatures in orthogonal and oblique cutting follow similar trends (Venuvinod & Lau, 1986).

Table 3. Analysed chemical composition of RHA steel produced by continuous casting route.

| EQUATION | MATERIAL | TOOL | CONFIGURATION | AUTOR |
|---|----------|--------------------|---------------|-------------------------|
| $T_{max}(K)$ $= 1623.49$ $+ .086 \alpha$ $- 0.031 \gamma$ $+ 0.7 V_c$ | 0.45 C | WC | Orthogonal | Fazil et al. (2004) |
| T $= 0.0174 V_c^{0.182}$ $t_1^{0.085} w^{0.040}$ $S_{ut}^{2.84}$ $k^{-2.9}$ | General | DNMG 15061 2 TN200 | Oblique | Rodríguez et al. (2011) |

During the machining process, the temperatures in the deformation zones increase due to the conversion of the material's plastic deformation energy into heat. The amount of strain energy produced is dependent on the thermo-mechanical behavior of the material, and it has been estimated that approximately 90% of this energy is converted into heat. Understanding this phenomenon is crucial to accurately validate the developed models (Barzegar & Ozlu, 2021; Komanduri & Hou, 2000; Rapier, 1954; Weiner, 2022).

In Figure 7, theoretical cutting temperature trends are shown as dots, and the values estimated with the models developed in this study are indicated by lines. For medium carbon steels, the temperature values estimated in this work are consistent with this theoretical reference.

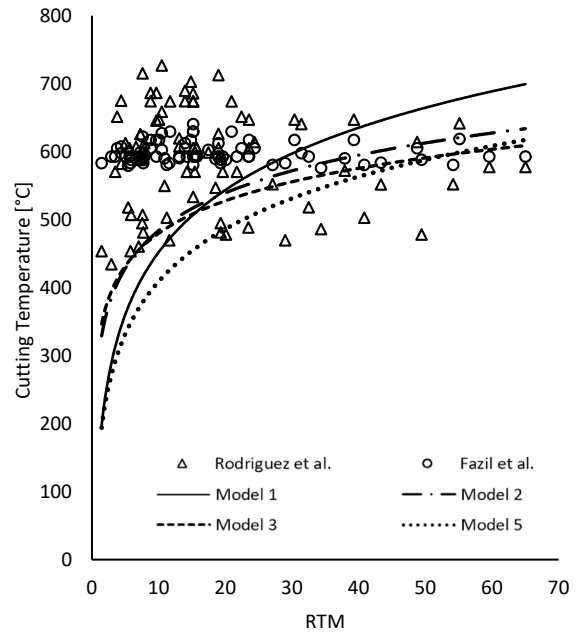
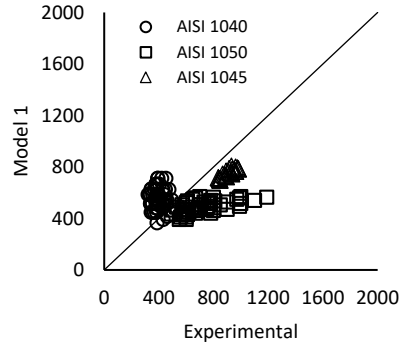


Figure 7. Comparison of models 1,2,3 and 5 with previously validated theoretical models (Fazil et al., 2014; Rodríguez et al., 2011).

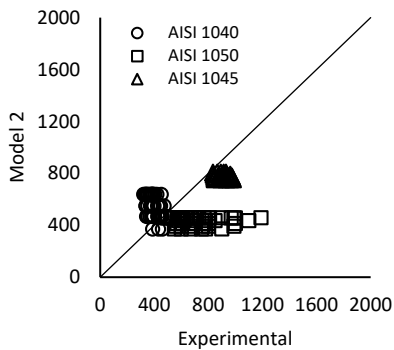
After validating the T_c evolution trends with R_{TM} (Phase A), the estimates obtained with Models 1-5 were compared with experimental results from a different source than the one used for modeling (Saglam et al., 2007). Figure 8 illustrates these results (Phase B). The experimental data used to validate the developed models were obtained by machining AISI 1040/1045/1050 steel with uncoated flat carbide tools. Table 4 presents the parameter ranges covered in this experimental data.

Table 4. Experimental parameter ranges used in the validation of the developed models.

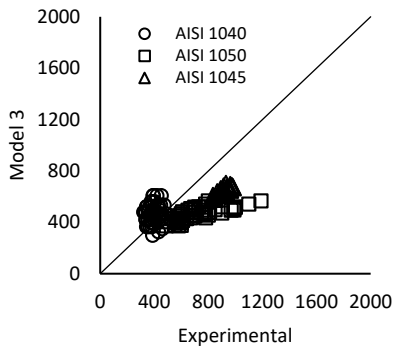
| MATERIAL | $V_c [m/min]$ | $t_1 [mm]$ | $\alpha [^\circ]$ $/\alpha_m [rad]$ | $w [mm]$ |
|-----------|---------------|---------------|--|----------|
| AISI 1040 | 75 - 236 | 0.2 | 0 - 20/ 1.570 - 1.222 | 1.5 |
| AISI 1045 | 100 - 200 | 0.2 | -5 / 1.658 | 0.6 - 1 |
| AISI 1050 | 60 - 300 | 0.1 - 0.15 | 3 - 11 / 1.518 - 1.379 | 3 |



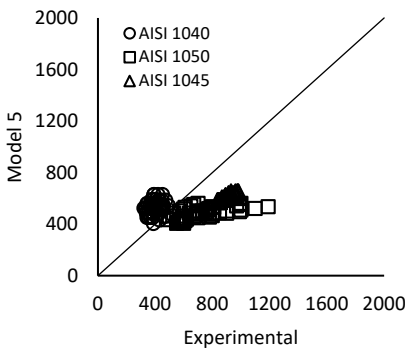
(a)



(b)



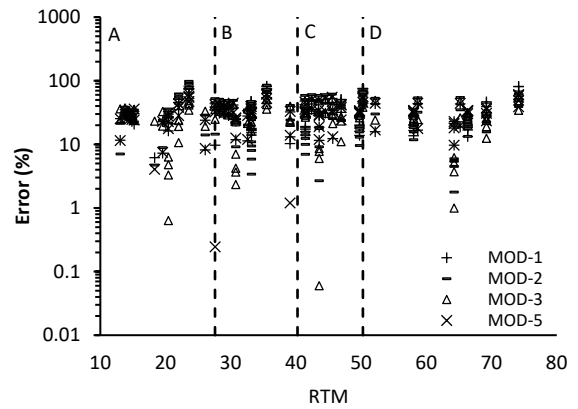
(c)



(d)

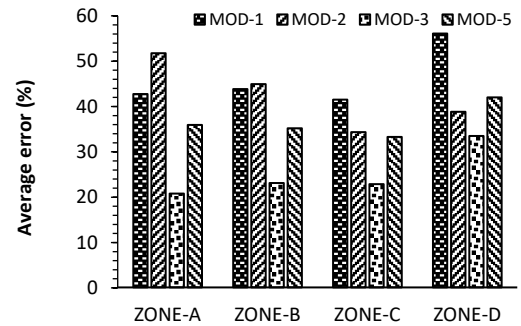
Figure 8 provides strong evidence that the models presented in this study consistently predict experimental temperature trends. The estimated temperatures are consistent with the carbon content in the different steels. To further investigate the efficacy of these models, a thorough error analysis was conducted, as depicted in Figure 9. It is important to highlight that this aspect of the validation process covers the range of medium carbon steels (AISI 1040-1045-1050) (Figure 9: (a)-(g)).

AISI 1040/1045/1050

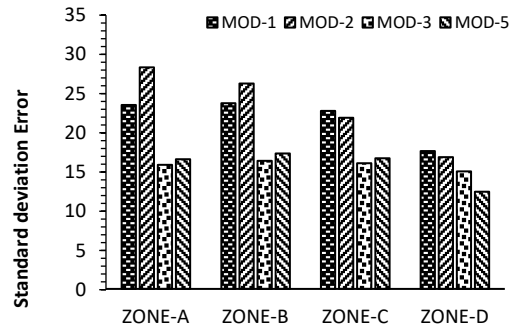


(a)

AISI 1040



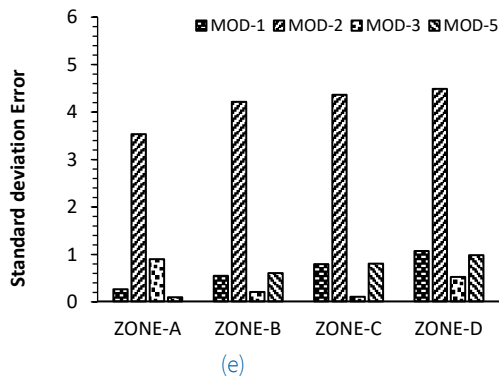
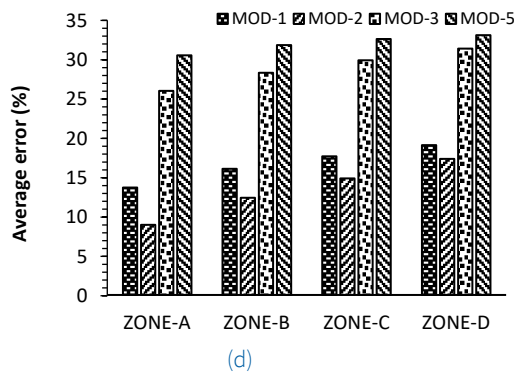
(b)



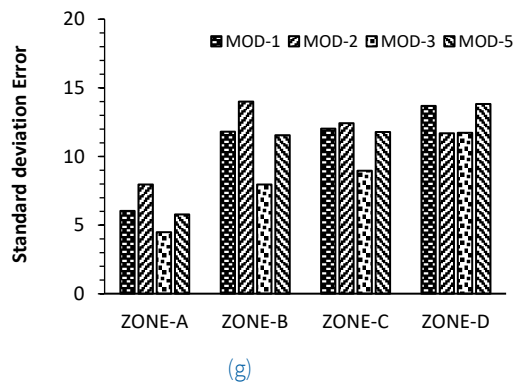
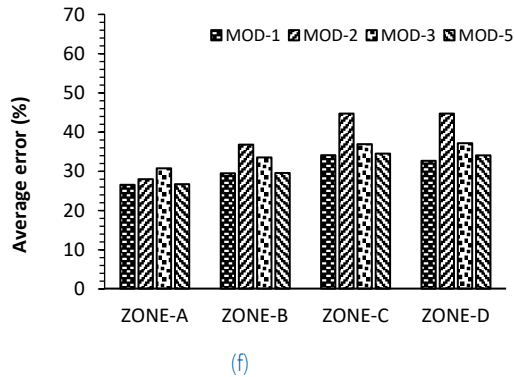
(c)

Figure 8. Validation of models developed with experimental data other than modeling data. (Al Huda et al., 2002; Barzegar & Ozlu, 2021; Saglam et al., 2007)

AISI 1045



AISI 1050



To analyze the error approximation for the developed models, the R_{TM} domain was segmented into four zones (A, B, C, D) based on quartiles. For each material analyzed, the average error of each model was calculated within each zone and presented in Figure 9 (b, d, f). Furthermore, the stability of the models was evaluated by examining the standard deviation of the error, as depicted in Figure 9 (c, e, g).

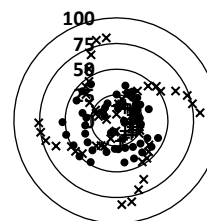
The developed models show deviations in their temperature predictions for steels with 0.4% and 0.5% carbon content. For 0.4% carbon, the models overestimate the temperature, while for 0.5%, they underestimate it. This confirms the consistency of the results, as machining temperatures in steel are related to carbon content-the higher the carbon content, the higher the cutting temperature. It also confirms the specificity of the models for steel with 0.45% carbon, with less error and greater stability in the estimates.

Table 4 outlines the experimental cutting conditions used to validate the models. Specifically, cutting of AISI 1040 steel was performed with a constant feed rate (t_1) and a constant depth of cut (w), while cutting of AISI 1045 steel was conducted with a constant feed rate (t_1) and a constant rake angle (α_m). For AISI 1050 steel, a constant depth of cut (w) was used.

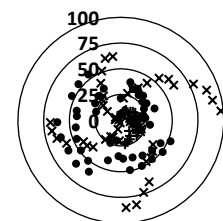
Models 3 and 5 demonstrated the highest level of accuracy in predicting the behavior of AISI 1040 steel when considering a constant feed rate (t_1) and depth of cut (w), with a standard deviation of less than 16%. These results align with the experimental conditions outlined in Table 4 and reinforce the effectiveness of these models for this specific application. For this material, all the experimental cutting temperatures were overestimated by the developed models.

For AISI 1045 steel, the most accurate predictions were obtained using model 2, which yielded a standard deviation of less than 4.5%, while model 1 achieved a standard deviation of less than 1%. The superior performance of model 2 can be attributed to the low cutting speed employed in the experimental conditions, which aligns with the modeling parameters.

For AISI 1050 steel, the most accurate predictions were produced by Model 1, while Model 3 proved to be the most stable. For this material, all the experimental cutting temperatures were underestimated by the developed models. Figure 10 provides a graphical representation of the validation results and the predictive capability of the models.



(a) MOD_1



(b) MOD_2

Figure 9. Error analysis in the validation of the models proposed in this work.

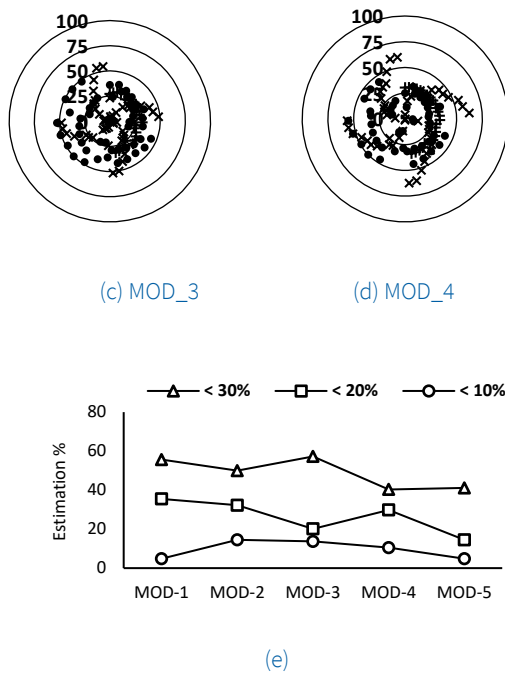


Figure 10. Effectiveness in the prediction of cutting temperatures.

After validating the models, it becomes possible to assess the impact of each variable V_c , t_1 , α_m and w on the estimation of cutting temperatures (T_c). The results indicate that the cutting speed (V_c), feed rate (t_1), and depth of cut (w) are the most influential variables in determining the values of cutting temperature.

The impact of the modified rake angle (α_m) on cutting temperature is most significant when the feed rate and depth of cut are low. This phenomenon relates to the energy transformation that occurs in the primary and secondary deformation zones. When the feed rate and depth of cut are increased, more material is deformed, resulting in a greater amount of thermal energy being transferred. Thus, cutting speed, feed rate, and depth of cut are the most influential variables in determining cutting temperature. Conversely, when the feed rate and depth of cut are small, the system becomes unstable, making temperature prediction more challenging.

Models 1 and 2 are the most reliable in predicting cutting temperatures, exhibiting maximum standard deviations of 16% for the most effective models. The validation process involving experimentally derived data was successful, yielding trends that were consistent with the experimental data. These findings demonstrate that regression models achieve the modeling objective.

3. Conclusions

In this study, five equations for predicting cutting temperature were developed using experimental data sourced from high-impact specialized literature. The experimental conditions involved orthogonal cutting of medium carbon steel using flat, uncoated carbide tools. The proposed equation structure allows modeling the influence of each cutting parameter on the cutting temperature. The modeling process was carried out using the multivariate linear regression method, and the statistical conditions were successfully verified, yielding statistically significant results. The validity of the proposed models was confirmed by comparing their predictions with both previously validated theoretical data and experimental results. The resulting models identify cutting speed V_c , feed rate t_1 , rake angle α_m , and depth of cut w as key variables for predicting cutting temperature and accurately reproduce both experimental and theoretical trends in the cutting temperature. All the parameters used in the modeling process have a significant influence, but the analysis indicates that V_c , t_1 , and w are the most influential parameters on cutting temperature, in that order. For low values of R_{TM} , the influence of cutting tool geometry is greater, making the influence of α_m on cutting temperature more significant when $t_1 < 0.1\text{ mm}$ and $w < 1\text{ mm}$. Predictions made using the developed models tend to underestimate cutting temperatures for carbon content higher than 0.45% and overestimate them for lower carbon content. All the developed models show an acceptable level of consistency in predicting temperatures for steel with 0.45% carbon, depending on the cutting conditions. However, Model 1 is more generally applicable across the range of modeling parameters.

Conflict of interest

The authors have no conflict of interest to declare.

Acknowledgements

Support from Universidad Técnica del Norte, Facultad de Ingeniería en Ciencias Aplicadas (FICA), is gratefully acknowledged.

Funding

This research received no external funding.

References

- Al Huda, M., Yamada, K., Hosokawa, A., & Ueda, T. (2002). Investigation of temperature at tool-chip interface in turning using two-color pyrometer. *J. Manuf. Sci. Eng.*, 124(2), 200-207. <https://doi.org/10.1115/1.1455641>
- Attanasio, A., Ceretti, E., Rizzuti, S., Umbrello, D., & Micari, F. (2008). 3D finite element analysis of tool wear in machining. *CIRP Annals*, 57(1), 61-64. <https://doi.org/10.1016/j.cirp.2008.03.123>
- Barzegar, Z., & Ozlu, E. (2021). Analytical prediction of cutting tool temperature distribution in orthogonal cutting including third deformation zone. *Journal of Manufacturing Processes*, 67, 325-344. <https://doi.org/10.1016/j.jmapro.2021.05.003>
- Battaglia, J. L., Cois, O., Puigsegur, L., & Oustaloup, A. (2001). Solving an inverse heat conduction problem using a non-integer identified model. *International Journal of Heat and Mass Transfer*, 44(14), 2671-2680. [https://doi.org/https://doi.org/10.1016/S0017-9310\(00\)00310-0](https://doi.org/https://doi.org/10.1016/S0017-9310(00)00310-0)
- Boothroyd, G. (1963). Temperatures in Orthogonal Metal Cutting. *Proceedings of the Institution of Mechanical Engineers*, 177(1), 789-810. https://doi.org/10.1243/PIME_PROC_1963_177_058_02
- Çakır, E., Özlü, E., Bakkal, M., & Budak, E. (2012). Modeling of temperature distribution in orthogonal cutting with dual-zone contact at rake face [Papers in Conference Proceedings]. Ecole Polytechnic. <https://research.sabanciuniv.edu/id/eprint/20790/>
- Chu, T. H., & Wallbank, J. (1998). Determination of the Temperature of a Machined Surface. *Journal of Manufacturing Science and Engineering*, 120(2), 259-263. <https://doi.org/10.1115/1.2830122>
- Ducobu, F., Rivière-Lorphèvre, E., & Filippi, E. (2013). Influence of the Material Behavior Law and Damage Value on the Results of an Orthogonal Cutting Finite Element Model of Ti6Al4V. *Procedia CIRP*, 8, 379-384. <https://doi.org/10.1016/j.procir.2013.06.120>
- Emamian, A. (2018). *The effect of tool edge radius on cutting conditions based on updated Lagrangian formulation in finite element method* (Doctoral dissertation). <https://macsphere.mcmaster.ca/handle/11375/22867>
- Fazil, M., Devan, R. J., & Prasad, K. (2014). *Finite Element Analysis of Turning AISI 1045 with Tungsten Carbide Tool and Prediction of Process Variables by varying the Turning Conditions*.
- Ghafarizadeh, S., Lebrun, G., & Chatelain, J.-F. (2016). Experimental investigation of the cutting temperature and surface quality during milling of unidirectional carbon fiber reinforced plastic. *Journal of Composite Materials*, 50(8), 1059-1071. <https://doi.org/10.1177/0021998315587131>
- Grzesik, W. (2006). Composite layer-based analytical models for tool–chip interface temperatures in machining medium carbon steels with multi-layer coated cutting tools. *Journal of materials processing technology*, 176(1-3), 102-110. <https://doi.org/10.1016/j.jmatprotec.2006.02.025>
- Kitagawa, T., Kubo, A., & Maekawa, K. (1997). Wear characteristics of various cutting tools in steel machining. In *Tribology Series* (Vol. 32, pp. 569-578). [https://doi.org/10.1016/S0167-8922\(08\)70483-8](https://doi.org/10.1016/S0167-8922(08)70483-8)
- Komanduri, R., & Hou, Z. B. (2000). Thermal modeling of the metal cutting process: Part I — Temperature rise distribution due to shear plane heat source. *International Journal of Mechanical Sciences*, 42(9), 1715-1752. [https://doi.org/10.1016/S0020-7403\(99\)00070-3](https://doi.org/10.1016/S0020-7403(99)00070-3)
- Lee, V. G., & Yeh, T. H. (2008). Sintering effects on the development of mechanical properties of fired clay ceramics. *Materials Science and Engineering: A*, 485(1), 5-13. <https://doi.org/10.1016/j.msea.2007.07.068>
- Lei, S., Shin, Y. C., & Incropera, F. P. (1999). Thermo-mechanical modeling of orthogonal machining process by finite element analysis. *International Journal of Machine Tools and Manufacture*, 39(5), 731-750. [https://doi.org/10.1016/S0890-6955\(98\)00059-5](https://doi.org/10.1016/S0890-6955(98)00059-5)
- Liu, C., He, Y., Wang, Y., Li, Y., Wang, S., Wang, L., & Wang, Y. (2020). Effects of process parameters on cutting temperature in dry machining of ball screw. *ISA Transactions*, 101, 493-502. <https://doi.org/https://doi.org/10.1016/j.isatra.2020.01.031>
- Mane, S., Karagadde, S., & Joshi, S. S. (2019). Study of Cutting Edge Radius Effect on the Cutting Forces and Temperature During Machining of Ti6Al4V. In *Advances in Computational Methods in Manufacturing: Select Papers from ICCMM 2019* (pp. 309-316). Springer Singapore. https://doi.org/10.1007/978-981-32-9072-3_26

- Maranhão, C., Silva, L. R., & Davim, J. P. (2013). Comportamento termo mecânico no micro-torneamento ortogonal do aço AISI 1045 (Ck45 - DIN): Simulação via elementos finitos e validação experimental. *Ciência & Tecnologia dos Materiais*, 25(1), 57-66. <https://doi.org/10.1016/j.ctmat.2013.12.006>
- Mutyalu, K. B., Reddy, V. V., Reddy, S. U. M., & Prasad, K. L. (2021). Effect of machining parameters on cutting forces during turning of EN 08, EN 36 & mild steel on high speed lathe by using Taguchi orthogonal array. *Materials Today: Proceedings*, 80, 2411-2415. <https://doi.org/10.1016/j.matpr.2021.06.374>
- Norouzifard, V., & Hamed, M. (2014). Experimental determination of the tool-chip thermal contact conductance in machining process. *International Journal of Machine Tools and Manufacture*, 84. <https://doi.org/10.1016/j.ijmachtools.2014.04.003>
- Pal, M., & Dasmahapatra, S. (2022). Estimation of cutting forces and tool tip temperature in turning operation with help of artificial neural network. *Materials Today: Proceedings*, 66, 1623-1632. <https://doi.org/10.1016/j.matpr.2022.05.251>
- Ramírez, P., F., Soldani, X., Loya, J., & Miguélez, H. (2017). A new approach for time-space wear modeling applied to machining tool wear. *Wear*, 390, 125-134. <https://doi.org/10.1016/j.wear.2017.07.015>
- Rapier, A. C. (1954). A theoretical investigation of the temperature distribution in the metal cutting process. *British Journal of Applied Physics*, 5(11), 400. <https://doi.org/10.1088/0508-3443/5/11/306>
- Rodríguez, J., Muñoz-Escalona, P., & Cassier, Z. (2011). Influence of cutting parameters and material properties on cutting temperature when turning stainless steel. *Revista de la Facultad de Ingeniería Universidad Central de Venezuela*, 26(1), 71-80.
- Saglam, H., Unsacar, F., & Yaldiz, S. (2006). Investigation of the effect of rake angle and approaching angle on main cutting force and tool tip temperature. *International Journal of Machine Tools and Manufacture*, 46(2), 132-141. <https://doi.org/10.1016/j.ijmachtools.2005.05.002>
- Saglam, H., Yaldiz, S., & Unsacar, F. (2007). The effect of tool geometry and cutting speed on main cutting force and tool tip temperature. *Materials & Design*, 28(1), 101-111. <https://doi.org/10.1016/j.matdes.2005.05.015>
- Tanaka, R., Yamane, Y., Sekiya, K., Narutaki, N., & Shiraga, T. (2007). Machinability of BN free-machining steel in turning. *International Journal of Machine Tools and Manufacture*, 47(12-13), 1971-1977. <https://doi.org/10.1016/j.ijmachtools.2007.02.003>
- Uçak, N., Aslantas, K., & Çiçek, A. (2020). The effects of Al₂O₃ coating on serrated chip geometry and adiabatic shear banding in orthogonal cutting of AISI 316L stainless steel. *Journal of Materials Research and Technology*, 9(5), 10758-10767. <https://doi.org/10.1016/j.jmrt.2020.07.087>
- Ulutan, D., Lazoglu, I., & Dinc, C. (2009). Three-dimensional temperature predictions in machining processes using finite difference method. *Journal of Materials Processing Technology*, 209, 1111-1121. <https://doi.org/10.1016/j.jmatprotec.2008.03.020>
- Umbrello, D., Filice, L., Rizzuti, S., Micari, F., & Settineri, L. (2007). On the effectiveness of Finite Element simulation of orthogonal cutting with particular reference to temperature prediction. *Journal of Materials Processing Technology - J MATER PROCESS TECHNOL*, 189, 284-291. <https://doi.org/10.1016/j.jmatprotec.2007.01.038>
- Umbrello, D., Filice, L., Rizzuti, S., Micari, F., & Settineri, L. (2007). On the effectiveness of finite element simulation of orthogonal cutting with particular reference to temperature prediction. *Journal of Materials Processing Technology*, 189(1-3), 284-291. <https://doi.org/10.1016/j.jmatprotec.2007.01.038>
- Verma, M. K., & Srivastava, A. (2022). Investigation about machining issues in turning process of EN-31 steel. *Materials Today: Proceedings*, 50, 2361-2364. <https://doi.org/10.1016/j.matpr.2021.10.238>
- Venuvinod, P. K., & Lau, W. S. (1986). Estimation of rake temperatures in free oblique cutting. *International Journal of Machine Tool Design and Research*, 26(1), 1-14. [https://doi.org/10.1016/0020-7357\(86\)90191-5](https://doi.org/10.1016/0020-7357(86)90191-5)
- Weiner, J. H. (2022). Shear-Plane Temperature Distribution in Orthogonal Cutting. *Transactions of the American Society of Mechanical Engineers*, 77(8), 1331-1336. <https://doi.org/10.1115/1.4014682>
- Yousefi, S., & Zohoor, M. (2019). Effect of cutting parameters on the dimensional accuracy and surface finish in the hard turning of MDN250 steel with cubic boron nitride tool, for developing a knowledge based expert system. *International Journal of Mechanical and Materials Engineering*, 14(1), 1. <https://doi.org/10.1186/s40712-018-0097-7>